Cooperative relaxations in amorphous polymers studied by thermally stimulated current depolarization

Bryan B. Sauer* and Peter Avakian
E.I. DuPont de Nemours and Company, Inc., Central Research and Development, Experimental Station, Wilmington, DE 19880-0356, USA
(Received 25 November 1991; revised 13 February 1992; accepted 21 March 1992)

Thermally stimulated current depolarization (t.s.c.) was used to study the relaxations in amorphous polymers including poly(ethyl methacrylate) (PEMA), poly(methyl methacrylate) (PMMA), polystyrene (PS), polycarbonate (PC) and polyarylate (PAR) over temperature ranges covering the β and α (glass transition) regions. A.c. dielectric was used to obtain activation energies (E_a) for PS and PC to verify the accuracy of those values determined by the t.s.c. thermal sampling method. At temperatures below the glass transition (T_g) the values of E_a were found to agree with those predicted using an activated states equation with a zero activation entropy. This is evidence of the localized, non-cooperative nature of the low temperature secondary β relaxations which are found to be characterized by a continuous variation of activation energies as a function of temperature. The measured values of E_a depart from the zero activation entropy curve and exhibit a prominent maximum at T_g. This behaviour is known to be due to an enhanced degree of cooperativity of segmental relaxations near T_g. The results indicate that the main advantage of the thermal sampling method is the high sensitivity and high temperature resolution for cooperative relaxations. For the polymers studied here, only PEMA and PMMA show a substantial population of cooperative relaxations more than 60°C below T_g. This is tentatively explained in terms of structural heterogeneity due to variable tacticity in the methacrylates. Compensation of the t.s.c. relaxation spectra plotted in Arrhenius or Eyring plots was found for all polymers to differing degrees. Some discussion of compensation is made in terms of independently measured values of the coefficient of thermal expansion.

(Keywords: amorphous polymers; thermally stimulated current; depolarization)

INTRODUCTION

The thermally stimulated current depolarization (t.s.c.) thermal sampling (t.s.) technique has been applied to polymers showing the capability of resolving complex dielectric relaxation spectra as a function of temperature[1-8] (ref. 1 reviews most work before 1986). These studies have illustrated the advantages of the programmable nature of the polarization sequence which allows one to excite only the specific transition of interest. In this study we present data obtained by the t.s. method with the aim of obtaining a more global view of relaxations in amorphous homopolymers as studied by this technique. Use of the proposed analysis scheme, although admittedly phenomenological, should facilitate more use of the technique for complicated systems in order to fully exploit the high resolving power which is the main strength of the t.s. method, especially in the case of overlapping transitions. Some of the present applications in this laboratory include the study of phase separated blends with overlapping transitions[9], highly crystalline linear aliphatic and fluorinated polymers with more than one 'cooperative' amorphous relaxation, and materials with broad or otherwise structured glass transitions such as those seen in crystallizable blends[10] or semicrystalline aromatic polymers[11,12]. The analysis strategy involves comparing the apparent activation energies (E_a) obtained from t.s. spectra with a zero activation entropy prediction[13], in order to assess the degree of cooperativity of the relaxation. It is known[14] that for cooperative amorphous relaxations (such as a glass transition) there is a sharp increase in E_a and a consequent departure from the zero activation entropy prediction[15]. Because of the high sensitivity of the t.s. method, one can resolve cooperative relaxations corresponding to high values of E_a even if the species are a minor fraction of the overall relaxing species.

Related to the sharp increase in E_a near the glass transition (T_g) is the occurrence of compensating Arrhenius relaxation curves coming to a focus in temperature–frequency space. Compensation is observed in many areas of chemical kinetics[16] and has been reported in several thermally stimulated current[1-8] and creep studies[4,5,17-20]. The compensation equation suggests that at the compensation point T_c, all relaxations occur at a single relaxation time τ_c. Some discussion and experimental evidence by Read[21], directly probing the compensation point in polypropylene[18] with low frequency mechanical measurements, have refuted the claim of a unique relaxation at T_c. Conformational entropy theories of relaxations[22-24] in the equilibrium state above T_g suggest that the cooperatively moving unit is largest at T_g and smaller at higher temperatures because more configurations (more free volume) are available.

*To whom correspondence should be addressed

0032-3861/92/245128-15
© 1992 Butterworth-Heinemann Ltd.

Predictions can also be made using these theories in the non-equilibrium glassy state below T_g (ref. 25). The theories suggest that the structural state in the glass should give rise to an Arrhenius dependence of relaxation times with the values of E_a increasing with temperature as the glassy structure approaches equilibrium[22–25]. Thus, this type of structural change in the non-equilibrium state can qualitatively explain the increasing values of E_a as one approaches T_g from the low T side and can also be used to explain compensation.

We also apply a relationship describing compensation in terms of material parameters following Eby[26], who has successfully modelled equilibrium mechanical relaxation data above T_g in terms of the isobaric volume coefficient of thermal expansion (α_l). While Eby's data were taken in the equilibrium polymer melt region, our compensating relaxation spectra are obtained in the glassy state at or below T_g. Still, we find some agreement with the proposed relationship although the range of the α_l values obtained is quite narrow. It is also known that there is an empirical correlation between $1/\alpha_l$ and T_g so the relationship of T_c, which occurs close to T_g, may be fortuitous for the case of the thermal sampling t.s.c. results.

We have devoted substantial effort to the characterization of relaxations using complementary techniques such as t.s.c. and a.c. dielectric in this report. In a few cases, including that of low temperature relaxations in oxidized polyethylene[27,28], it was shown that E_a determined from t.s. data compares well with other techniques[4,13,29]. In some cases the values of E_a determined by the t.s. method for glass transitions are a factor of 1.5 to 4 times lower than those obtained by other relaxation methods[30–32]. It is shown here that the values of E_a obtained by the t.s. method for several polymers agree with those obtained from a.c. dielectric measurements, not only for low temperature relaxations but also for higher temperature ones such as the glass transition with some corrections for the different measurement frequency. Thus, we feel that the accuracy of the values is substantiated, giving some confidence that the t.s. data can be used to quantify the nature of cooperative and non-cooperative relaxations.

EXPERIMENTAL

Materials

Films were between 0.05 and 0.3 mm thick with areas of $\sim 50\ mm^2$ for t.s.c. and $\sim 350\ mm^2$ for a.c. dielectric. Films for t.s.c. were stored under vacuum ($\sim 10^{-4}$ mbar) at 30°C to avoid water vapour sorption. Bisphenol-A polycarbonate (PC) (Lexan®, General Electric) was obtained in 0.075 mm sheets with $M_w \sim 37\,000$. Two different types of poly(methyl methacrylate) (PMMA) were used. A narrow distribution PMMA (M_w 480 000, $M_w/M_n = 1.1$; Pressure Chem. Co., Pittsburgh, PA, USA) was a solvent precipitated sample. This PMMA and the polystyrene (PS) (M_w 1 860 000, $M_w/M_n = 1.12$, Pressure Chem. Co.) were the only samples that were solvent cast. The solvent cast films were annealed under vacuum at T_g to remove residual solvent. Another sample of PMMA (Poly Science, cat. no. 4553) had a rather broad molecular weight distribution (M_w 100 000, $M_w/M_n = 2$, determined by g.p.c.). Films of PMMA, poly(ethyl methacrylate) (PEMA) and PS were melt pressed at 170°C between sheets of polyimide (which acts as a release film) sandwiched between two glass slides. The polyarylate (PAR) studied ($M_w \sim 25\,000$) was an amorphous aromatic polyester which was a reaction product of bisphenol-A and a mixture of iso and terephthalic acids. PEMA was synthesized by dissolving 100 cm^3 of ethyl methacrylate in 400 cm^3 of ethyl acetate and then adding 0.1 g of benzoyl peroxide as the initiator. The product was refluxed for 4 h and then precipitated by methanol and washed and dried before pressing into films.

Methods

A.c. dielectric. The a.c. dielectric experiments were performed in the parallel plate geometry using sputter coated films. A Hewlett Packard LCR meter (model 4274A) was used to measure the capacitance C and dissipation factor ($\tan\delta = \varepsilon''/\varepsilon'$) of the sample at 11 frequencies in the range 10^2–10^5 Hz from $-190°C < T < 250°C$ at a heating rate of 1.5°C min^{-1}. The real ε' and imaginary ε'' components of the dielectric permittivity were calculated using:

$$\varepsilon' = dC/(\varepsilon_o A), \qquad \varepsilon'' = \varepsilon' \tan\delta \tag{1}$$

where d is the sample thickness, ε_o is the permittivity of vacuum (8.854×10^{-12} F m^{-1}), A is the metallized electrode area (350 mm^2), and δ is the loss angle.

Thermally stimulated currents. The t.s.c. spectrometer (Solomat Instruments, Stamford, CT, USA) was used over the temperature range −180 to 300°C. A Faraday cage shielded the sample and a cold finger and a heating coil were used for temperature control. Before the experiment was started, the sample cell was evacuated to $\sim 10^{-4}$ mbar and then flushed with 1.1 bar of high purity He (grade 5.5, 99.9995%, keen compressed gas). Parallel plate electrodes were used in the majority of the experiments with the upper plate spring-loaded to maintain electrical contact during thermal cycling. Further improvements in electrode contact were made by sputter coating both sides of the film with gold/palladium. Some low temperature results were obtained by painting both sides of the film with colloidal silver and attaching wires. The sample was suspended next to the thermocouple in the cell to obtain accurate temperature values. The silver painted electrodes could not be used above ~180°C because of decomposition.

Both 'global' t.s.c. spectra and thermally cleaned (t.s.) spectra were obtained. For global t.s.c. experiments the film was first polarized by a static electric field ($E \sim 100$–2000 kV m^{-1}) over a temperature range from the polarization temperature T_p down to the 'freezing temperature' T_o, with cooling during polarization at approximately 30°C min^{-1} to freeze in dipolar orientation. Then the field was turned off and the sample was short circuited as the temperature was increased from T_o at 7°C min^{-1} to a final temperature $T_f (\geqslant T_p)$. The depolarization current was due to a convolution of all dielectrically active relaxations excited over the temperature and frequency range probed.

Spectra in the t.s. mode[27,33] were obtained by applying the polarizing field for 4 min over a narrow range of temperatures from T_p to $T_p - 5°C$, depolarizing for 2 min at $T_p - 5°C$ with the field off, and then quenching at 30°C min^{-1} with the field off to about 40°C below T_p. The depolarization spectrum due to a narrow distribution of relaxations was then measured upon reheating at 7°C min^{-1} to values about 40°C above T_p.

BACKGROUND

van Turnhout[34,35] has shown that t.s.c. is in many ways similar to low frequency dielectric loss experiments. The depolarization current (J) measured by t.s.c. can be related to the dielectric strength (or dielectric increment, $\Delta\varepsilon$) measured for a given transition[34,35]:

$$\Delta\varepsilon = \frac{1}{\varepsilon_0 E}\int_{t_0}^{\infty} J/A\, dt \qquad (2)$$

A comparison of the integrated t.s.c. peak with the dielectric increment determined from a.c. dielectric data by taking the difference between the value of ε' at high frequency and the value at low frequency, shows good agreement between the two techniques for the α and β relaxations in several polymers[36].

The equivalent measurement frequency of t.s.c. is[34,35]:

$$f = E_a/(2\pi s R T^2) \qquad (3)$$

where s is the inverse heating rate and R is the ideal gas constant (1.987 cal mol^{-1} K^{-1}). For our studies the equivalent frequency is generally on the order of 10^{-3} Hz. This low measurement frequency leads to enhanced resolution of the various relaxations, yet the experiments can be performed in a short amount of time with high sensitivity.

T.s. of the t.s.c. spectra is performed by polarizing the sample over a narrow temperature window (1–5°C), quenching, and then measuring the depolarization over a ~70°C range. The relaxation time spectra $\tau(T)$ is obtained using the standard method[37]:

$$\ln \tau(T) = \ln\left\{\int_{T_0}^{T} J(T)\, dT\right\} - \ln J(T) \qquad (4)$$

where T_0 is the initial temperature of the t.s. depolarization scan. The t.s. spectrum is partially integrated numerically up to T to determine each value of $\tau(T)$. Since this is only an approximate method of determining $\tau(T)$, values of $\tau(T)$ are only obtained up to the maximum of the t.s. peak. The values of $\tau(T)$, typically spanning the range 10^1 s $< \tau < 10^4$ s, are plotted *versus* reciprocal temperature as a Bucci curve[37] on an Arrhenius plot. The Arrhenius equation relates the relaxation time constant τ to the barrier height E_a (or apparent activation energy):

$$\tau(T) = \tau_0 \exp(E_a/RT) \qquad (5)$$

where τ_0 is the pre-exponential factor.

The t.s. spectra can also be analysed directly in current–temperature space using the theory developed by Fröhlich[27,28,38]:

$$J(T) = P_0/\tau_0 \exp\{-E_a/RT - s/\tau_0 \int_{T_0}^{T} \exp(-E_a/RT')\, dT'\} \qquad (6)$$

where P_0 is a constant related to the initial polarization and T_0 is the initial temperature of the depolarization scan. To facilitate fitting of the experimental profile using the Fröhlich model, an approximate form of the integral on the right-hand side is used[39]. Using a single value of E_a in equation (6) generates t.s. spectra which are quite asymmetric as a function of temperature while the experimental data are quite symmetric. This is remedied by assuming that there is a slight breadth to the distribution of activation energies[13,27,28]. Surprisingly, it is also possible to generate symmetric t.s. spectra by inputting a few narrowly spaced but discrete values of E_a:

$$J(T) = \sum_{i=1}^{n} a_i J(T, E_{a,i}) \qquad (7)$$

where n is usually 2 or 3, a_i are normalized weighting factors, $E_{a,i}$ is the ith activation energy and $J(T, E_{a,i})$ is calculated using equation (6). The mean value of E_a obtained by fitting the data in this manner was shown to be the same as that calculated using the Bucci method[13].

RESULTS AND DISCUSSION

Global t.s.c. spectra

Global t.s.c. spectra are characterized by a broad spectrum of relaxations similar to low frequency dielectric loss experiments. Other differences arise because t.s.c. is a direct current measurement and accumulation of charges at buried interfaces (i.e. Maxwell–Wagner) or injection of charges near the electrode surfaces leads to additional high temperature transitions, which are not detected by a.c. experiments[34]. For the amorphous materials studied here, PEMA and PMMA are the most sensitive to impurities such as adsorbed water. These impurities lead to space charge injection near electrode surfaces giving rise to transitions above T_g referred to as ρ transitions. T.s.c. spectra for PEMA and the monodisperse PMMA are given in *Figure 1* and are generally consistent with earlier data[34]. The films were dried close to T_g under vacuum (10^{-4} mbar) for ~1 day. The peak temperatures for the β and α transitions are summarized in *Table 1* where β is a secondary low temperature relaxation occurring below the glass transition (α). The values of T_g measured by t.s.c. are comparable to those measured by d.s.c. at the same scan rate, as is indicated in *Table 1*.

The results for PS, PC and PAR are given in *Figure 2* showing a sharp T_g peak (α) in each case. The films were all approximately 0.07 mm thick with metallized

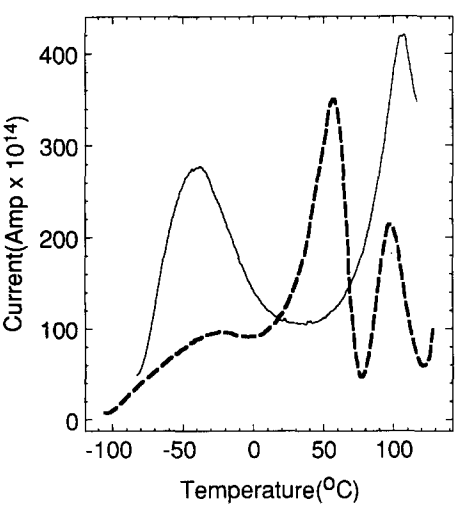

Figure 1 Global t.s.c. spectra of current *versus* temperature for PEMA (– – –) and PMMA (——) with a polarization temperature, $T_p = 130$°C, $E = 750$ kV m^{-1} and sample area, $A = 78$ mm^2. The transition temperatures are given in *Table 1*

Table 1 Transition temperatures obtained by d.s.c. and t.s.c. at the same scan rates

	β (t.s.c.) (°C)	T_g (t.s.c.) (°C)	T_g (d.s.c.) (°C)
PEMA	−27	57	54
PMMA[a]	−37	108	107
PMMA[b]	−38	106	109
PS	–[c]	105	104
PC	−140	148	147
PAR	−119	178	178

[a]Monodisperse PMMA sample with $M_w = 480\,000$
[b]Polydisperse PMMA sample with $M_w = 100\,000$
[c]No β relaxation was observed for PS

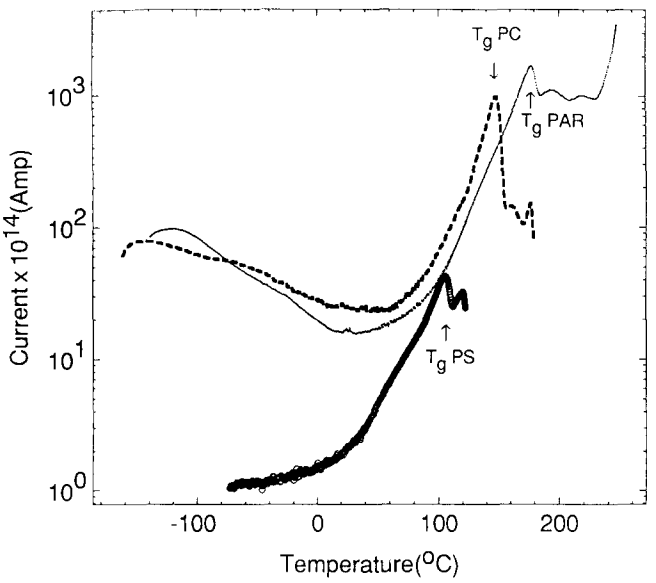

Figure 2 Global t.s.c. spectra for PC, PAR and PS with $E = 2000\ \text{kV m}^{-1}$, $A = 78\ \text{mm}^2$. $T_p = 160, 180$ and 120°C for PC, PAR and PS, respectively. The transition temperatures are given in *Table 1*. The small bumps in the signal above T_p are due to spontaneous stress relaxation and not dipolar relaxations

areas of 78 mm^2 so the relative signal strength can be compared quantitatively. The data in the T_g region for PC are consistent with those presented earlier[40]. The secondary relaxation temperatures (β) are listed in *Table 1*. The β peak intensities are significantly lower than the α relaxation intensities. In the case of PS, no β relaxation was detected as expected[14]. It has been suggested that the β relaxation in PS is only detected dielectrically if the sample contains polar impurities[14]. The signal is generally more than an order of magnitude lower for PS than for the other polymers due to the weak dipoles involved. There is a small peak around −80°C for PC. It is known that the results in the β relaxation region for PC are sensitive to adsorbed water[41].

Quenching below T_g leads to incomplete volume relaxation. Subsequent annealing for extended times just below T_g allows slow densification (or physical ageing) to occur as equilibrium is approached. van Turnhout[36] has shown that t.s.c. is very sensitive to ageing effects in the case of poly(vinyl chloride). Physical ageing effects here play a minor role during the short ageing times required for some of the experiments. Replicate runs obtained after annealing for a short time (10–20 min) just below T_g, showed no evidence of ageing.

Since we will focus on the region around T_g in terms of t.s. experiments in the next section, it is of interest to understand more fully the nature of the ρ relaxation. The ρ relaxation always occurs above T_g although the exact nature of the relaxation seems to vary depending on the polymer. For semicrystalline polymers and for other materials with multiphase morphologies, charge trapping at interfaces or Maxwell–Wagner polarization phenomena are likely[34–36]. For the amorphous materials investigated here, it is also possible that the effects are related to conductive impurities, injected space charges and other electrode effects. Some discussion of other high temperature viscoelastic relaxations has also been made for PMMA with respect to the liquid–liquid transition (T_{ll})[32]. For many polymers[42] T_{ll} generally occurs at $T_g + 0.2T_g$ (with T_g in K). Thermal annealing of the polymer in the vicinity of T_{ll} is necessary to detect T_{ll} in many cases[42,43]. For our quenched polymer films, no substantial evidence of T_{ll} was detected by d.s.c. and we did not systematically study the high temperature region further. Vacuum treatment of PEMA and PMMA to remove water had a large effect on the ρ peak, indicating that it may be related to mobile charge carriers[34,35]. Further data are given below.

The ρ peak in PEMA at ~115°C is well separated from the T_g peak at 57°C (*Figure 3*). Annealing at 55°C under 10^{-4} mbar gives rise to a strong decrease in the ρ peak at ~115°C, while the β and α transitions are not influenced. In the case of PMMA, the ρ peak at ~118°C overlaps with T_g (*Figure 4*). Drying at 105°C results in a strong decrease in the ρ peak (*Figure 4*) but, as in the case of PEMA, it is difficult to remove completely even at T_g where water has significant mobility. van Turnhout[36] has performed an interrupted t.s.c. experiment where the PMMA film was first polarized and then removed from the cell and sectioned into three layers. Next a depolarization scan was obtained for each of the sections. It was found that for the outer sections,

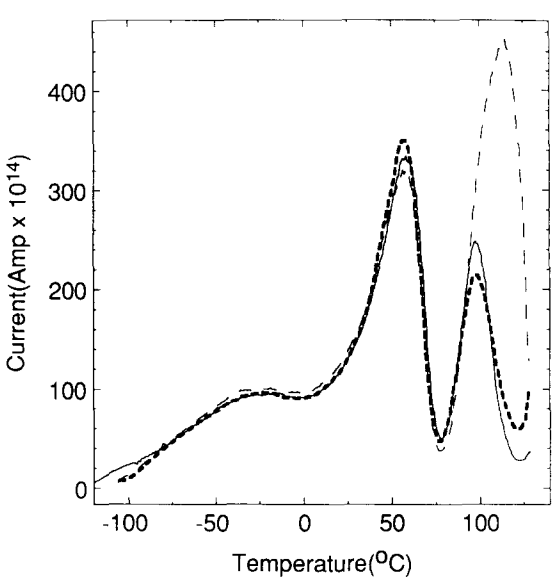

Figure 3 Influence of vacuum drying on PEMA; global t.s.c. spectra were taken with $T_p = 120$°C, $E = 750\ \text{kV m}^{-1}$, $A = 78\ \text{mm}^2$ and sample thickness ≈0.55 mm. The sample was stored under ambient conditions (25°C, r.h. ~40%) for 3 days resulting in a strong ρ peak due to adsorbed water (– – –). After vacuum treatment for 30 min (——) and 120 min (– – –) at 10^{-4} mbar and $T = 55$°C, a significant decrease in the intensity of the ρ peak was observed at ~115°C

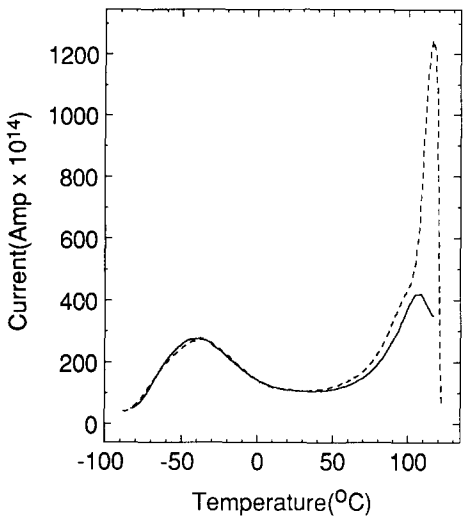

Figure 4 Effect of water on PMMA; global t.s.c. spectra were taken with $T_p = 130°C$, $E = 750\ kV\ m^{-1}$, $A = 78\ mm^2$ and sample thickness ≈ 0.2 mm. The PMMA film was solvent cast from methylene chloride, dried under N_2 at atmospheric pressure to remove volatiles by heating slowly to 105°C and then holding for 30 min, then immediately transferred to the t.s.c. sample chamber (——). Next, the sample was stored under ambient conditions (25°C, r.h. ~40%) for 12 days resulting in the growth of a strong ρ peak at 120°C (– – –) and a conversion of the glass transition peak to a shoulder

which were adjacent to the original polarizing electrodes, previously injected space charges contributed to a strong ρ peak, while no such peak was seen in the spectra from the inner section. This suggests that the ρ relaxation is due to free charge carriers injected near the electrode surface and also explains why vacuum treatment well below T_g, to remove water from the surface but not necessarily the bulk, is sometimes effective in suppressing some of the surface charging effects in the cases where water plays a role.

Additional peak assignments are obtained by noting the dependence of the current maxima on the magnitude of the polarization field strength (E)[34,35,40]. For relaxations above T_g, the current does not always scale linearly with E[13,34,35,40] while for relaxations at T_g and below, the majority of the literature indicates that scaling with E holds. This linear dependence is one indication that the processes are dipolar, although it is not always a definitive test because Maxwell–Wagner charging at buried interfaces is sometimes 100% efficient and can look like a dipolar process[34,35]. T.s.c. spectra taken at three different polarization voltages are given in *Figure 5a* for PEMA. A strong dependence on E is seen at all temperatures. To determine the exact dependence with E, the same data are plotted as current divided by E at the bottom of *Figure 5* showing that the β, α and ρ peak intensities are well normalized by this procedure. Minor deviations in *Figure 5b* are seen for $E = 75\ kV\ m^{-1}$ due to ohmic conductivity which starts at temperatures above 90°C. Ohmic conductivity is spontaneous current flow; it is independent of E and can be easily subtracted.

For PMMA with some residual water (*Figure 4*), the intensity of the ρ relaxation at 120°C also scaled with E if the maximum temperature was kept below 130°C. The intensity did not change significantly during four to five t.s.c. scans up to 130°C, even though at these temperatures one would expect some diffusion of water out of the film into the dry helium environment. Further experiments need to be performed to understand these features more fully. As expected, the current also scales with E for PS, PC and PAR in terms of the α and β transitions, with the exception of PS for which the β relaxation was not detected[14].

Comparison with a.c. dielectric results

A.c. dielectric data were collected for PS and PC in order to compare with the t.s.c. results. The Arrhenius relaxation maps[14] of measurement frequency (f) *versus* temperature from the loss peak $(1/T_{max})$ are shown in *Figures 6* and *7* for the β and α transitions, respectively. T.s.c. peak temperatures at an equivalent frequency of $\sim 10^{-3}$ Hz are also included in *Figures 6* and *7*. For PC

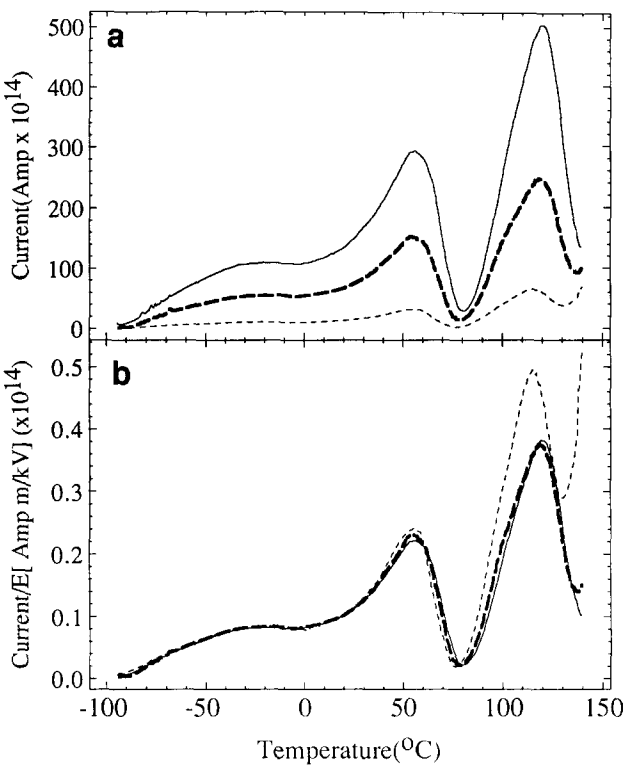

Figure 5 (a) Dependence of current on polarization field strength (E) for PEMA. (b) The measured current is normalized by dividing by E: the data indicate that all three relaxations scale with E. The deviation of the high temperature data $(T > 80°C)$ taken at the lowest field strength is due to the d.c. conductivity background (see text). Values of E: – – –, $75\ kV\ m^{-1}$; – – –, $375\ kV\ m^{-1}$; ——, $750\ kV\ m^{-1}$

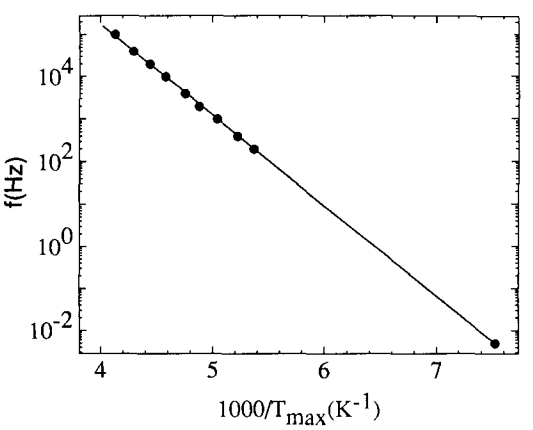

Figure 6 Arrhenius plot of $\log(f)$ *versus* the reciprocal peak temperature $1/T_{max}$ for the β relaxation in PC for both t.s.c. (0.005 Hz) and a.c. dielectric data. The slope gives an activation energy of 9.8 ± 0.2 kcal mol^{-1}

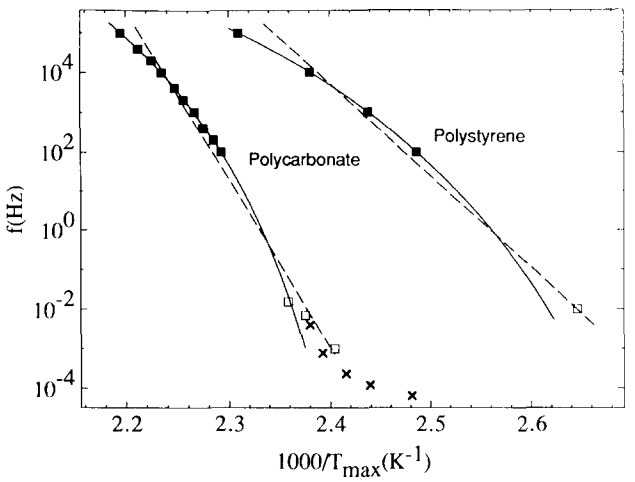

Figure 7 Arrhenius plot of $\log(f)$ *versus* the reciprocal peak temperature $1/T_{max}$ for the $\alpha(T_g)$ relaxation in PC and PS. The points between 10^2 and 10^5 Hz are a.c. dielectric data. □, T_gs obtained from global t.s.c. maxima at different heating rates; ×, data from isothermal depolarization measurements (see text). The activation energy estimated from the Arrhenius line (– – –) is 195 kcal mol^{-1}. ——, WLF fit to the high frequency data. The deviation from the equilibrium WLF curve at low frequencies is due to non-equilibrium effects associated with incomplete volume relaxation

in *Figure 6* the data for the β relaxation are linear over almost 8 orders of magnitude in frequency, giving a slope of $E_a = 9.8$ kcal mol^{-1}. The data can also be plotted as an Eyring plot of f/T_{max} *versus* $1/T_{max}$. This type of plot is also linear, as observed by Chatain *et al.*[33], even over the wide frequency range (8 decades) covered here, giving an Eyring activated states enthalpy of $\Delta H^{\ddagger} = 9.5$ kcal mol^{-1}. The slightly lower value for the Eyring activation enthalpy ($\Delta H^{\ddagger}$) is expected because $\Delta H^{\ddagger}$ and E_a are related by[44]:

$$E_a = \Delta H^{\ddagger} + RT \tag{8}$$

Thus, there is no difference between the Eyring and Arrhenius models for this application. The magnitude of the Arrhenius prefactor (τ_0) is in many cases unrealistic and often reaches values less than 10^{-30} s. To obtain more physically reasonable parameters, Eyring's activated states equation is used[33]:

$$f = 1/(2\pi\tau) = kT/(2\pi h)\exp(-\Delta H^{\ddagger}/RT)\exp(\Delta S^{\ddagger}/R) \tag{9}$$

where k is Boltzmann's constant, h is Planck's constant and $\Delta S^{\ddagger}$ is the activated states entropy. The intercept of an Eyring plot of f/T_{max} *versus* $1/T_{max}$ is then

$$k/(2\pi h)\exp(\Delta S^{\ddagger}/R)$$

from which $\Delta S^{\ddagger}$ can be calculated.

For the α transition or T_g in *Figure 7*, the relaxation map from 10^2 to 10^5 Hz exhibits significant curvature for PC and PS. Three low frequency points are from t.s.c. spectra taken at different scan rates. Isothermal depolarization data are also included and will be discussed below. The curvature at high frequencies is analysed using the Vogel equation which is equivalent mathematically to the Williams–Landel–Ferry (WLF) equation:

$$-\ln f = a_1 + a_2/(T - T_\infty) \tag{10}$$

where $f = 1/(2\pi\tau)$ is the measurement frequency and a_1, a_2 and T_∞ are fitted parameters. T_∞ is the critical temperature where the relaxation becomes infinitely slow. Non-linear regression gives the solid curve for PC with $a_1 = -28.6$, $a_2 = 1136$ and $T_\infty = 389$ K. For PS the fitted parameters are $a_1 = -27.0$, $a_2 = 1541$ and $T_\infty = 333.5$ K. Even though the values of E_a are frequency dependent, we have estimated some average value, as indicated by the dashed lines in *Figure 7*, resulting in $E_a = 195 \pm 20$ kcal mol^{-1} for PC and $E_a = 107 \pm 15$ kcal mol^{-1} for PS.

Three lower frequency points for PC were obtained from t.s.c. spectra taken at different scan rates including 15°C min^{-1} ($f = 0.015$ Hz), 7°C min^{-1} ($f = 0.007$ Hz) and 1°C min^{-1} ($f = 0.001$ Hz) giving the three open squares. The error is greater for the 15°C min^{-1} scan, possibly because of temperature gradients in the cell.

Some additional low frequency measurements were made by the isothermal dielectric depolarization technique using the Solomat instrument. The sample was polarized for 5 min at constant temperature and the depolarization current was then measured as a function of time also at constant temperature. The time dependent current was converted to a loss peak in the frequency domain by the Hamon approximation as described by Jonscher[45]. These preliminary isothermal results are plotted in *Figure 7* for PC indicating that there is an inflection in the relaxation map at $\sim 10^{-1}$ Hz.

It is evident that the Vogel cuve, fitted to the high frequency data, does not extrapolate well through the low frequency data although the deviation is rather small for PS. Due to incomplete volume relaxation after quenching below T_g, the polymer is frozen in a non-equilibrium state. For a material quenched from $T > T_g$ to $T < T_g$, which induces an isostructural state representative of that seen at elevated temperatures, it has been shown that the viscosity (proportional to the relaxation time τ) deviates significantly from the curve for the equilibrium fluid at low temperatures and is characterized by a lower activation energy[46]. Both the equilibrium and non-equilibrium states are well described by the Adam-Gibbs theory[25]. The departure from the equilibrium curve and subsequent lowering of the value of E_a has been shown previously for a variety of polymers[47]. The crossover from the equilibrium liquid to the non-equilibrium solid is around 10^{-1} Hz for PC. Another feature of the Adam-Gibbs theory is that the relaxation behaviour in the isostructural state below T_g is predicted to be Arrhenius. This is supported by the t.s.c. relaxation data presented below and thus the entropy theories may provide a framework for understanding compensation in the glassy state which is a rather controversial issue[3,21]

T.s.c. thermal sampling

PEMA. To illustrate some features of the thermal peak cleaning or t.s. experiment, representative t.s. spectra are given in *Figure 8* along with the global t.s.c. for PEMA. At temperatures well below T_g, each t.s. spectrum is characterized by a narrow distribution of relaxations with essentially a single value of E_a. The Gaussian function, which has no theoretical justification, is fitted to the t.s. spectra (dashed curves) to indicate any asymmetry in the spectrum (*Figure 8*). The deviation of the Gaussian fits on the low temperature side of the t.s. peaks for spectra taken in the vicinity of T_g (*Figure 8*) indicates that the relaxation is characterized by multiple values of E_a and shows up as deviation from

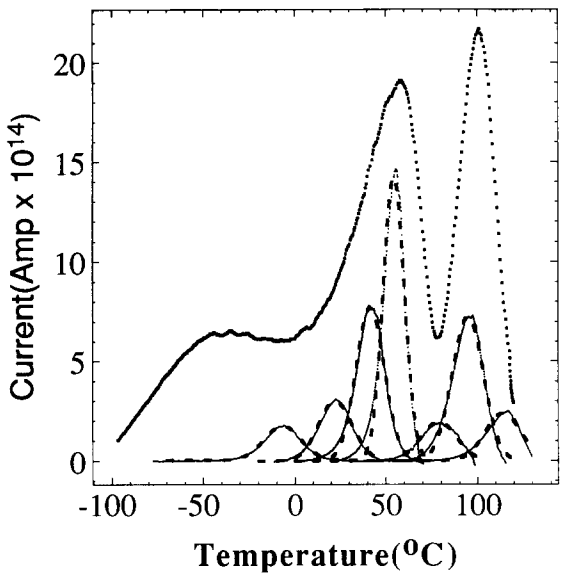

Figure 8 Global t.s.c. spectrum (upper curve, $T_p = 120°C$) and t.s. spectra for PEMA with corresponding Gaussian fits using $E = 100\ kV\ m^{-1}$ and $A = 30\ mm^2$. T_p (°C) for t.s. spectra (from left to right): −20; 10; 30; 45; 70; 90; 110. The Gaussian fits (– – –) are included only to indicate the range over which the Bucci plot is linear (see text)

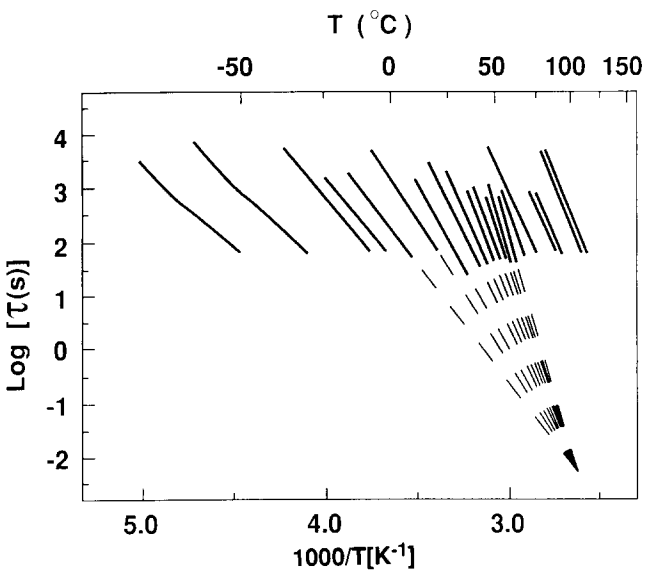

Figure 9 Arrhenius plots of Bucci curves for PEMA of the calculated realxation times (τ) *versus* $1/T$ obtained by fractional integration of the t.s. spectra. The polarization temperatures are approximately the centre point of each line and the peak maxima occur near the high T end of each Arrhenius line. The extrapolated compensation point is indicated by the dashed lines coming to a focus

Arrhenius behaviour. This asymmetry can be seen more clearly in *Figure 12* for PEMA and *Figure 13* for PC, both of which were polarized in the vicinity of T_g. The PC data will be discussed in more detail later.

Several Bucci curves obtained by fractional integration of each t.s. spectrum using equation (4) are shown in *Figure 9*, with the slopes proportional to E_a. The compensating lines which come to a focus in this plot will be discussed later. Unlike other techniques, such as the a.c. dielectric technique discussed earlier, the relaxation dynamics are determined at any temperature by the thermal sampling method giving a characterization of E_a over the complete temperature range. The apparent activation energies are plotted in *Figure 10* and show a sharp maximum at $T_g = 57°C$. The zero activation entropy line in the plot is discussed below in the context of equation (11).

We interject here to discuss one other method which has been used for the analysis of t.s. spectra. Instead of numerical integration, the t.s. spectra can be fitted directly using the Fröhlich method[27,28,38]. The Fröhlich analysis of a representative t.s. spectrum taken in the vicinity of T_g for PEMA is shown in *Figure 11*. The single E_a Fröhlich fit (equation (6)) is poor and gives a value of E_a which is too low (*Table 2*). A Gaussian fit is also shown, illustrating the asymmetry on the low temperature side of the peak which indicates a low E_a process. A fit was performed using equation (7) with three values of $E_{a,i}$ and three values of a_i to account for the asymmetric

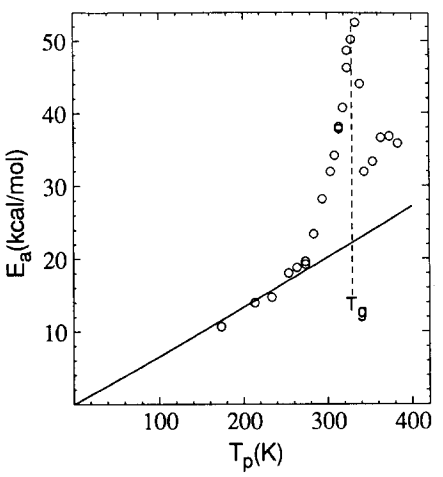

Figure 10 Apparent activation energies E_a for PEMA *versus* polarization temperature T_p. The values of E_a are from the slopes of the Arrhenius lines in *Figure 9* and the solid curve was calculated using the activated states equation with no adjustable parameters and $\Delta S^{\ddagger} = 0$ and $f = 5 \times 10^{-3}$ Hz

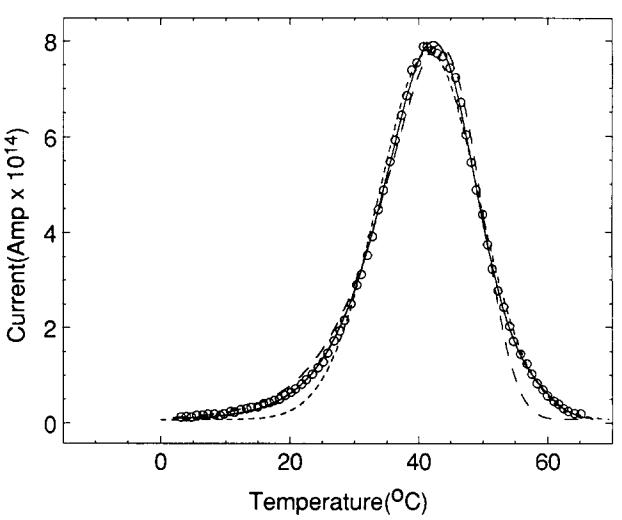

Figure 11 A representative thermally cleaned t.s.c. spectra for PEMA obtained in the vicinity of T_g using $T_p = 30°C$. ○, Experimental data; — —, Fröhlich fit, single E_a; ——, Fröhlich fit, distributed E_a; – – –, Gaussian curve. Parameters obtained from the distributed Fröhlich fit are discussed in the text. A narrow distribution of activation energies with mean values similar to those obtained from the Bucci plots (see text) is obtained. The low temperature deviation of the experimental data from the Gaussian curve indicates that there is a slower relaxing species

Table 2 Fröhlich analysis of thermally cleaned PEMA spectra

T_p (°C)	$E_{a,1}$ (kcal)	a_1 (%)	$E_{a,2}$ (kcal)	a_2 (%)	$E_{a,3}$ (kcal)	a_3 (%)	E_a[a] (kcal)	E_a[b] (kcal)
−20[c]	17.40	30	17.66	40	18.32	30	16.7	18.4
10[c]	21.80	30	21.86	40	22.65	30	19.1	23.4
30[d]	30.66	47	31.20	41	32.0	12	26.7	31.5

[a]Obtained from the Fröhlich fit with one activation energy
[b]Obtained from Bucci analysis
[c]The three normalized amplitudes (a_i) were fixed at 30, 40 and 30%
[d]The normalized amplitudes were allowed to vary in the fit because the t.s. spectrum was asymmetric

nature of the spectrum. As expected, the fitted values of the normalized amplitudes indicate an asymmetric distribution which is given in *Table 2*. The values of $E_{a,i}$, which correspond to the peak intensity region, are still close together with a deviation of less than ±2%. Because numerical analysis is performed without any weighting factors, the Bucci analysis by fractional integration is more sensitive to the asymmetric nature of the spectra in terms of extracting the low E_a process. The Fröhlich method, as we apply it, weighs the data around the peak quite heavily and is rather insensitive to the low temperature tail. The asymmetry in the t.s. spectra in the vicinity of T_g was found to varying degrees for all polymers. The resulting curvature in the Bucci plots is sometimes quite pronounced (see discussion of PC data).

Representative t.s. spectra at temperatures well below T_g and their best fits are given in *Figure 12*. The experimental spectra are symmetric but a single E_a fit results in an unsatisfactory fit of the data. The distributed E_a fit was performed using equation (7) and five parameters: τ_o, $E_{a,1}$, $E_{a,2}$, $E_{a,3}$ and one amplitude. Non-linear regression indicated a very narrow distribution in the three values of $E_{a,i}$ (<2% variation) with the mean value the same, within experimental error, as that obtained by the Bucci method (*Table 2*). A symmetric distribution was assumed for this distributed E_a fit of the data in *Figure 12*, where the normalized amplitudes a_1, a_2, a_3 were fixed at 30%, 40% and 30%, respectively. This normalized amplitude distribution was chosen arbitrarily and a good fit could be obtained for a variety of distributions. In fact, using only two activation energies in a five parameter fit, which includes τ_o, $E_{a,1}$, $E_{a,2}$, a_1 and a_2, also results in a good fit. The important point is that regardless of the distribution of a_i, a narrow spectrum of activation energies describes the data well. For the spectra at $T_p = -20$°C and 10°C shown in *Figure 12*, the spread in the three activation energies obtained from each fit is less than ±2% (*Table 2*). This is a general feature of the sub-T_g t.s. spectra for the other polymers analysed by the Fröhlich method.

The values of E_a can be compared with theoretical predictions in order to categorize the various relaxations as being cooperative or non-cooperative. Starkweather[15,48] has rearranged the activated states equation (9) to give:

$$E_a = \Delta H^{\ddagger} + RT = RT[22.92 + \ln(T/f)] + T\Delta S^{\ddagger}$$
$$= RT[24.76 + \ln(T\tau)] + T\Delta S^{\ddagger} \quad (11)$$

The solid curve in *Figure 10* was calculated using equation (11) with the activated states entropy ($\Delta S^{\ddagger}$) set equal to zero, a frequency of 5×10^{-3} Hz, and no other adjustable parameters. Far enough below T_g, the activation energies agree with the zero entropy prediction (*Figure 10*). It has been shown that low temperature secondary relaxations, studied by classical relaxation methods, also agree with the zero entropy prediction for a variety of polymers[15,48], because of the localized and non-cooperative nature of the motions. For cooperative amorphous relaxations, such as glass transitions, it was shown that the data deviated significantly from the $\Delta S^{\ddagger} = 0$ prediction[15]. A substantial departure from the zero entropy line is seen in *Figure 10* starting approximately 50°C below T_g for PEMA with E_a maximizing at T_g. Above T_g the data are not as reproducible but the qualitative trend indicates that it drops rapidly. The magnitude of the maximum in E_a at T_g (*Figure 10*) is consistent with the reported literature[49] which gave E_a as approximately 50 kcal mol^{-1} for the glass transition although the lower temperature β relaxation for PEMA is known to merge with the α transition at frequencies >1 Hz.

Polycarbonate. The low temperature tail corresponding to a low E_a process is even more exaggerated in *Figure 13* for PC polarized at 140°C which is close to T_g (148°C). The t.s. spectra are more asymmetric for PC than PEMA near T_g because of the extremely high values of E_a at T_g for PC. The features shown in *Figure 13* are independent of the t.s. polarization window width for windows ranging from 1 to 5°C. The low temperature tail corresponds to the region where the Arrhenius plot deviates from linearity. For example, the results of integrating six t.s. spectra taken near T_g for PC, including the one shown in *Figure 13*, are presented in an Arrhenius plot (*Figure 14*). The curvature (or inflections) are not artifacts and are directly related to tails on the low temperature side of the t.s. peaks. At $T_p = 130$°C the Bucci curve in *Figure 14* is linear but for the three curves very close to $T_g = 148$°C (i.e. $T_p = 140$, 150 and 155°C), there is an inflection at ~148°C. The steeper slope region corresponds to the points closer to the peak of the t.s. spectra. The inflection occurs because of the way the thermal sampling method is applied. This non-Arrhenius behaviour near T_g is a consequence of the t.s. depolarization scan where the temperature is varied

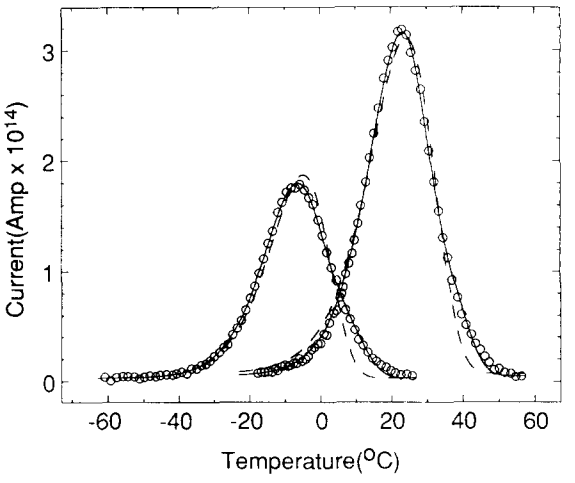

Figure 12 Representative t.s. spectra for PEMA obtained in the region well below T_g using $T_p = -20$°C and 10°C. ○, Experimental data; — —, Fröhlich fit, single E_a; ——, Fröhlich fit, distributed E_a. Parameters obtained from the distributed Fröhlich fit are discussed in the text and indicate a narrow distribution of activation energies with mean values similar to those obtained from the Bucci plots (see text)

across T_g. It is evident that relaxations representative of both low and high activation energy processes are detected in the same scan. Below T_g, low E_a relaxations are detected which correspond to the 'glassy state', and high E_a relaxations are detected at T_g and above. The inflection at T_g had been qualitatively simulated by taking into account the details of the applied t.s. pre-polarization sequence as a function of time and temperature for an inorganic glass[46].

The entire set of Bucci curves for PC is plotted in *Figure 15*. T.s. spectra obtained in the low temperature range from −150°C to 130°C are symmetric and result in linear Bucci curves. The slopes increase quite slowly and over part of the range the lines are almost parallel until one approaches T_g.

The activation energies are summarized in *Figure 16*. As discussed in the context of *Figure 14*, two values of E_a are extracted from the curved Bucci plots giving rise to two values for some T_ps in the vicinity of T_g. The results for PC are significantly different from those obtained for the methacrylates because the values of E_a for PC follow the $\Delta S^{\ddagger} = 0$ curve in *Figure 16* up to within ~20°C of T_g before increasing sharply. As was discussed above, a.c. dielectric studies on this material were performed to confirm the absolute values of the activation energies determined by t.s.c. The value of E_a for the β relaxation from *Figure 6* is plotted as the cross in *Figure 16* at 133 K (−140°C) showing good agreement. The value of $E_a = 195$ kcal mol^{-1} from the approximate

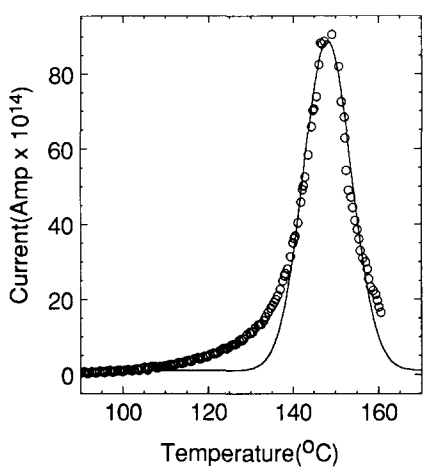

Figure 13 T.s. spectrum for PC illustrating the low temperature tail in the vicinity of T_g (148°C). The spectrum was taken at $E = 2000$ kV m^{-1} and $T_p = 140$°C. The deviation of the experimental data from the Gaussian curve on the low temperature side is more dramatic in this case and significant curvature in the Arrhenius curves (*Figure 14*) occurs at about the point where the deviation starts

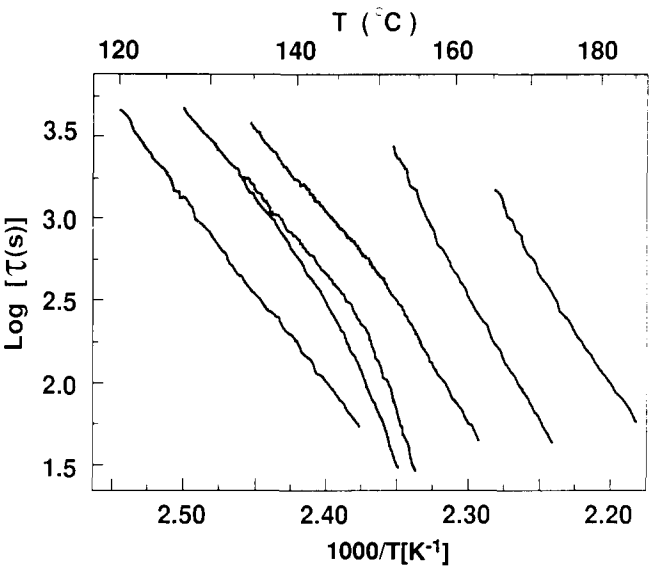

Figure 14 Arrhenius plots of integrated t.s. spectra showing non-Arrhenius behaviour in the vicinity of T_g for PC. T_p (°C) (from left to right): 130; 140; 150; 155; 165; 180. The inflection is due to the presence of a lower E_a process below T_g

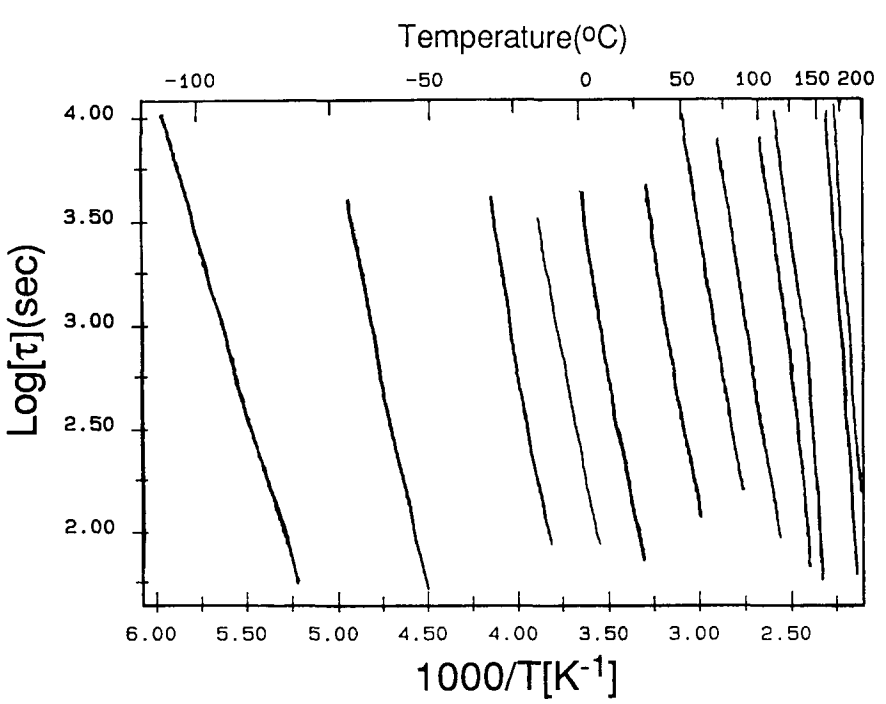

Figure 15 Arrhenius plots for PC over a wider temperature range. T_p (°C) (from left to right): −90; −60; −20; 0; 20; 50; 75; 100; 130; 150; 180; 190

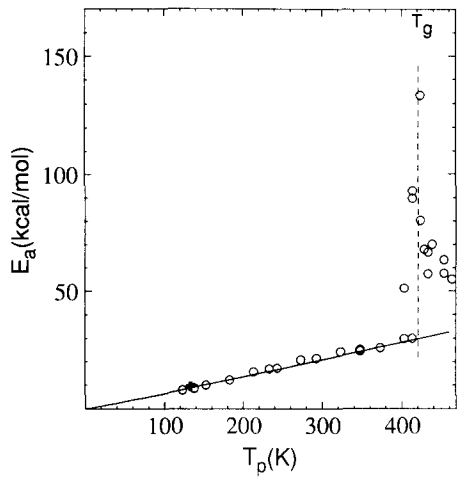

Figure 16 Apparent activation energies E_a *versus* T_p for PC. The dark cross at 133 K is from the relaxation map in *Figure 6* for the a.c. dielectric data. The solid curve was calculated using the activated states equation with no adjustable parameters and $\Delta S^{\ddagger} = 0$ and $f = 5 \times 10^{-3}$ Hz

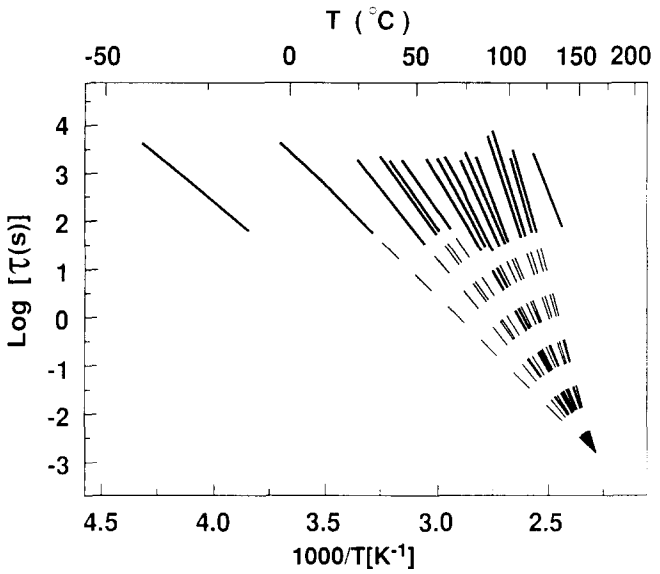

Figure 17 Arrhenius plots for PMMA of the calculated relaxation times (τ) *versus* reciprocal temperature obtained by integration of the t.s. spectra. The polarization temperatures are approximately the centre point of each line and the peak maxima occur near the high T end of each Arrhenius line. The extrapolated compensation point is also indicated (see text)

Arrhenius line in *Figure 7* is higher than the peak activation energy (134 kcal mol^{-1}) determined by t.s.c. at T_g. Taking into consideration the curvature in the Arrhenius plot, the estimated value of E_a at 10^{-2} Hz, taken as the tangent to the line in *Figure 7*, gives a value between 110 and 140 kcal mol^{-1} which is roughly consistent with the peak value in *Figure 16*.

PMMA. Bucci or Arrhenius plots of integrated t.s. spectra are given in *Figure 17* for the polydisperse PMMA sample. The data are similar to those obtained for PEMA with the slopes increasing monotonically up to T_g. The activation energies obtained from the slopes are plotted *versus* T_p for the monodisperse and polydisperse PMMA samples (*Figure 18*) showing no significant difference. The values of E_a are somewhat higher than those determined previously[30,32] for various PMMA samples near T_g. The values of E_a start to depart from the zero activated states entropy prediction at about ~290 K which is 90°C below T_g (380 K). The values above T_g are less reproducible from sample to sample because the ρ relaxation overlaps with T_g to a certain degree. The ρ relaxation is generally characterized by a significantly lower E_a than T_g and it is easy to resolve T_g from other non-cooperative relaxations by this method.

PS and PAR. Activation energies are plotted in *Figure 19* for PS and PAR indicating that E_a maximizes at T_g. The Bucci curves are similar to those shown in *Figure 17* for PC with respect to the curvature seen close to T_g. The value of $E_a = 76$ kcal mol^{-1} for PS at T_g is consistent with reported literature values[14,50] of $E_a = 79$ kcal mol^{-1} for atactic PS and also falls in the range of ~50 to 100 kcal mol^{-1} given by Saito and Nakajima[47]. It is slightly lower than the value of 107 kcal mol^{-1} estimated by the dashed line in *Figure 7* but similar to the case of PC discussed above; some discrepancy is expected because of the different frequencies used. The β relaxation is not

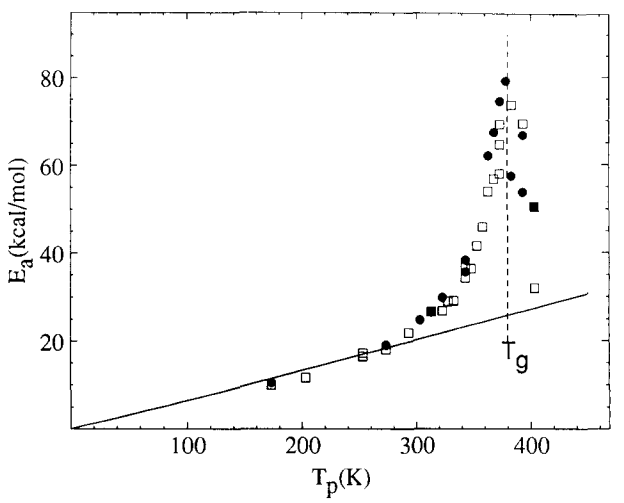

Figure 18 Apparent activation energies E_a *versus* T_p for polydisperse (□) and monodisperse (●) PMMA. Both materials have the same T_g as measured by d.s.c. The solid curve was calculated with the activated states equation with no adjustable parameters and $\Delta S^{\ddagger} = 0$ and $f = 5 \times 10^{-3}$ Hz

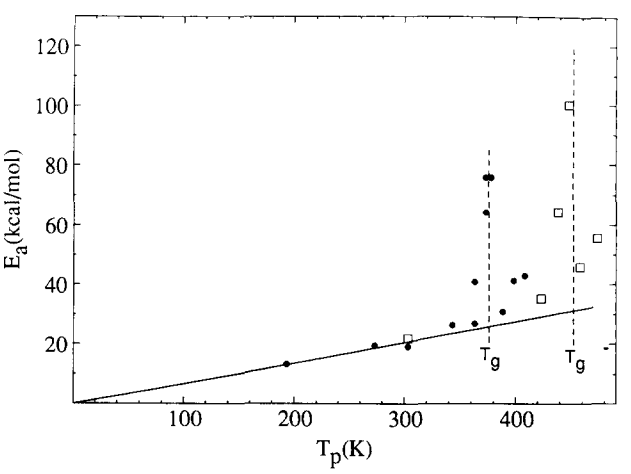

Figure 19 Apparent activation energies E_a *versus* T_p for PAR (□) and PS (●). The solid curve was calculated using the activated states equation with no adjustable parameters and $\Delta S^{\ddagger} = 0$ and $f = 5 \times 10^{-3}$ Hz

active dielectrically for PS. The values of E_a for PS and PAR roughly agree with the $\Delta S^{\ddagger} = 0$ curve below T_g, consistent with the other polymers studied.

Compensation

Compensation is observed in many areas of chemical kinetics[16] and has been reported in several t.s.c. studies[1–8,17–20,28,30–33]. It has been suggested that at the compensation point T_c, all relaxations occur at a single relaxation time τ_c but Read[21] has refuted this claim. This is not surprising since polymer relaxations are strongly moderated by quite complex interactions with their local environments.

Eby[26] has successfully modelled the compensation of equilibrium mechanical relaxation data above T_g in terms of the isobaric volume coefficient of thermal expansion of the polymer liquid (α_l). Compensation is generally determined from relaxation spectra taken in the vicinity just below T_g in the polymer glass by t.s.c. This is in the region where the glass is not in equilibrium because of incomplete volume relaxation. One purpose of this section is to present experimental data to compare with some of the proposed relationships which relate compensation to material properties. Besides the relationship used by Eby, it has been suggested[52] that compensation may be described in terms of the change in $\alpha(\Delta\alpha = \alpha_l - \alpha_s)$ which occurs when crossing the glass transition from solid (subscript s) to liquid (subscript l).

Just below T_g. For the materials studied here, only PEMA and PMMA show compensation over a wide temperature range. Compensation to a 'lesser' degree occurs near T_g for most polymers because of the increase in E_a associated with the glass transition. For many polymers the glass transition is sharp and compensation is only observed over a narrow temperature range (10–20°C) (see *Table 3* and references cited therein). For PC and PAR in this paper, the high activation energies (>100 kcal mol^{-1}) lead to inflections in the Arrhenius curves at T_g (i.e. *Figure 14* for PC) so compensation is very speculative. Our estimate of the compensation point for PC from *Figure 14* is included in *Table 3* along with other literature data for polymers with very narrow transitions.

Compensation is defined in terms of the linear dependence of E_a with the logarithm of the pre-exponential factor τ_o. Later we present an algebraically similar form in terms of the activated states enthalpy and entropy. Representative data are shown in *Figure 20* for PEMA. The compensation point is defined in frequency–temperature space by the two phenomenological parameters: the compensation temperature T_c and the compensation frequency or relaxation time, $(f_c = 1/(2\pi\tau_c))$:

$$\tau_o = \tau_c \exp(E_a/RT_c) \tag{12}$$

Substituting equation (12) into equation (5) gives the compensation equation:

$$\tau(T) = \tau_c \exp[E_a(1/T - 1/T_c)/R] \tag{13}$$

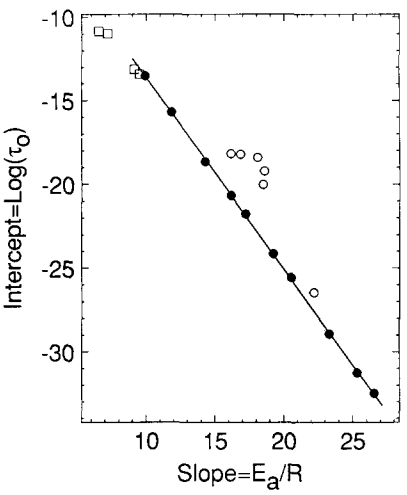

Figure 20 Arrhenius parameters for PEMA plotted as intercept (log τ_0) *versus* slope (E_a/R) to indicate the region of compensation. The linear points indicate the region of compensation. Ranges of T_p (°C): □, −60 to −10; ●, 0–60; ○, 65–110

Table 3 Relationship of compensation in the vicinity of T_g to the coefficient of thermal expansion

		τ_c (s)	T_c (°C)	ΔH_o (kcal mol^{-1})	Range of T_p (°C)	$\alpha = 1/(4T_c)^a$ $\times 10^4$(K^{-1})	$\alpha_l{}^b$ $\times 10^4$(K^{-1})	$\alpha_s{}^b$ $\times 10^4$(K^{-1})
Polymers	PEMA	6.8×10^{-3}	108 ± 5	19 ± 1	0–55	6.6	6.5[c]	3.1[d]
compensating	PMMA	1.6×10^{-3}	164 ± 5	20 ± 1	20–105	5.7	5.9[c]	2.7[d]
over wide T range	LCP1[e]	2.8×10^{-6}	188	20	−10 to 85	5.4	4.9[f]	1.56[f]
Polymers	PC	20	150		130–145	5.9	6.3[c]	2.1[c]
compensating	PS[g]	3	140		85–105	6.1	5.8[c]	2.4[c]
over narrow	PVC[h]	22	84		69–76	7.0	6.5[d]	2.35[d]
T range	PP[i]	0.1	23		−33 to −3	8.4	4.7/8.0[d]	2.4[d]

[a] Values calculated using $\alpha = 1/(T_cK_c)$ where T_c is the compensation temperature and a value of $K_c = 4$ was chosen arbitrarily (see text)
[b] Values for the volume coefficient of thermal expansion for the polymer liquid (α_l) and glass (α_s) were obtained from the references indicated
[c] Ref. 56
[d] Ref. 55
[e] Amorphous (~98%) aromatic main chain liquid crystalline copolyester, unpublished t.s.c. data
[f] Ref. 57
[g] Ref. 1
[h] Poly(vinyl chloride), ref. 4
[i] Polypropylene, ref. 3

From equation (12) it is evident that the slope of a plot of $\ln(\tau_0)$ *versus* E_a/R is the reciprocal compensation temperature ($1/T_c$) and the intercept is the compensation frequency (τ_c). The sharply increasing nature of E_a with temperature departing from the zero entropy line for PEMA (*Figure 9*) and PMMA (*Figure 17*) leads to these compensating lines. For PS[1] and PVC[4] compensation over a narrow temperature range has been found by obtaining t.s. spectra using very closely spaced polarization temperatures. The data for PEMA covering the range 0°C up to $T_g = 55$°C compensates extremely well, as indicated by the linear relationship in *Figure 20*, giving $T_c = 108 \pm 5$°C and $\tau_c = 6.8 \times 10^{-3}$ s, the latter corresponding to a compensation frequency of $f_c = 23$ Hz (*Table 3*). As discussed above, where the values of E_a follow the zero entropy prediction, the slope is changing so slowly that the Arrhenius lines are essentially a series of parallel lines, such as in the case of PC (*Figure 15*).

Secondary relaxations. We feel that compensation should be absent for all polymers in the region of low temperature secondary (non-cooperative) relaxations although one can always force three or four lines to compensate over a narrow temperature range, due to experimental uncertainty and the length of the extrapolation. We have calculated theoretical Arrhenius curves of relaxation times to simulate the experimentally determined compensation plots, assuming that the values of E_a agree with the zero entropy prediction (e.g. the solid line in *Figure 16* as predicted by equation (11)). From this calculation we conclude that compensation should occur at $\log \tau_c \sim -27$, which indicates that if one wishes to determine this compensation point from the data one would have to extrapolate the experimental data, which only covers three decades from $1 < \log \tau < 4$, approximately 28 decades. This extrapolation is out of the experimental range of accuracy and shows that any proposed compensation point in the range of $-1 < \log \tau_c < -10$, associated with non-cooperative low temperature relaxations well below T_g, is probably due to experimental error.

Activated states equation applied to compensation. The Arrhenius pre-exponential factors (τ_0) obtainded from the intercepts of Arrhenius plots are generally on the order of 10^{-10} to 10^{-35} s (*Figure 20*). These extremely small values of τ_0 are not physically reasonable. One can cast the same data in terms of an alternative thermodynamic model keeping in mind that the information is still limited by the complexity of the system and the lack of experimental verification of the activated states equation as it is applied to this analysis. In the Eyring analysis one plots $\ln(\tau T)$ *versus* $1/T$ instead of $\ln \tau$ *versus* $1/T$, thus defining a new intercept ($\tau_{0,\text{Eyring}}$) which is related to the activation entropy by:

$$\Delta S^{\ddagger} = -R(\ln \tau_{0,\text{Eyring}} + 23.76) \qquad (14)$$

As discussed in the context of *Figure 6*, $\ln(\tau T)$ or $\ln(\tau)$ *versus* $1/T$ plots are just equivalent ways of looking at the same data. The values of $\Delta S^{\ddagger}$ and $\Delta H^{\ddagger}$ for PEMA are plotted in *Figure 21* with the analogous Arrhenius parameters plotted in *Figure 20*. There is no direct algebraic relationship of $\tau_{0,\text{Eyring}}$ and the Arrhenius τ_0 although they differ by about a factor of $\ln T$. The relationship of the slopes is given by equation (8); for the Eyring plot the slope is $\Delta H^{\ddagger}$ and for the Arrhenius plot it is E_a.

As discussed above, Eby[26] found that the ratio $\Delta S^{\ddagger}/\Delta H^{\ddagger}$, determined from mechanical relaxation experiments of the glass transition, correlates with the coefficient of thermal volume expansion α_l for the polymer 'fluid' using the empirical relationship:

$$\Delta S^{\ddagger} = \Delta H^{\ddagger} \alpha_l K_c \qquad (15)$$

Eby found qualitative agreement with independently measured values of α_l for several polymers using the value proposed previously by Keyes[53] of $K_c = 4.0$. It is important to note that all of these measurements were made in the equilibrium fluid region just above either a glass transition or a transition which exhibits glass-transition-like behaviour (high activation energy process). Substituting equation (15) into the activated states equation (9) gives a compensation equation[33] that is mathematically equivalent to equation (13):

$$\tau(T) = h/(kT) \exp[\Delta H^{\ddagger}(1/T - \alpha K_c)/k] \qquad (16)$$

where the compensation temperature is now defined as $\alpha K_c = 1/T_c$.

Generally an additional factor is needed to explain the non-zero intercept of the experimental $\Delta S^{\ddagger}$ *versus* $\Delta H^{\ddagger}$ plots (e.g. *Figures 21* and *22*). Thus, we arbitrarily modify equation (15):

$$\Delta S^{\ddagger} = \Delta S^{\ddagger}_o + \Delta H^{\ddagger} K_c \alpha \qquad (17)$$

The intercept $\Delta S^{\ddagger}_o$ at $\Delta H^{\ddagger} = 0$ falls in the range of -0.035 to -0.05 kcal K^{-1} mol^{-1} for PEMA and PMMA, as found in previous work[33]. We do not attribute any significance to the intercepts because the values of $\Delta S^{\ddagger}_o$ depend on the activated states pre-factor and the absolute accuracy of this has not been substantiated.

We have also determined the x-intercept to be $\Delta H^{\ddagger}_o = 20 \pm 3$ kcal mol^{-1} at $\Delta S^{\ddagger} = 0$ for all polymers (e.g. *Figures 21* and *22* and *Table 3*). It is not surprising that the intercept, $\Delta H^{\ddagger}_o$, is independent of the material studied. Assuming $\Delta S^{\ddagger} = 0$, equation (11) indicates that:

$$\Delta H^{\ddagger}_o = \Delta G^{\ddagger} = RT \ln[\tau k T/h] = RT[23.76 + \ln(\tau T)] \qquad (18)$$

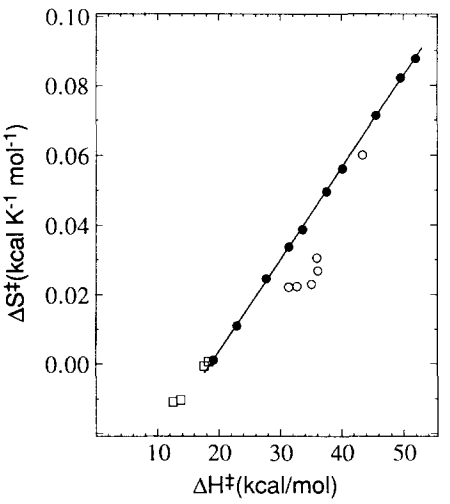

Figure 21 Activated states entropy ($\Delta S^{\ddagger}$) plotted *versus* the entropy ($\Delta H^{\ddagger}$) for PEMA. The linear points indicate the region of compensation. Ranges of T_p (°C): □, −60 to −10; ●, 0–60; ○, 65–110

There are no independent variables in equation (18) since τ is generally around 20 s, which explains the single value of $\Delta H_o^{\ddagger}$. The temperature at which $\Delta S^{\ddagger}$ becomes zero is about 290 K for all the polymers studied here by t.s.c.

Other comments on activated states analysis. At this point we make one additional comment on the pitfalls of the activated states analysis as applied to compensation of t.s.c. data. One can take the values from *Figures 21* and *22* and re-calculate the free energy ($\Delta G^{\ddagger} = \Delta H^{\ddagger} - T\Delta S^{\ddagger}$) as was proposed previously[54]. This is a cyclical exercise and the values are invariably determined to be the same as those defined by the Eyring equation:

$$\Delta G^{\ddagger} = \Delta H^{\ddagger} - T\Delta S^{\ddagger} = RT\ln[\tau kT/h] = RT[23.76 + \ln(\tau T)] \quad (19)$$

Keeping in mind that τ is constrained to ~ 100 s because of the equivalent frequency of the measurement (equation (3)), $\Delta G^{\ddagger}$ adds no new information because it is the same for all materials. Since the log term in equation (19) varies slowly with temperature, $\Delta G^{\ddagger}$ can be approximated as being nearly linearly dependent on T so it always increases monotonically with T, even across the glass transition where other parameters (E_a or $\Delta H^{\ddagger}$ and $\Delta S^{\ddagger}$) are varying rapidly.

Relationship to thermal expansion coefficient. Returning to the question of the relationship of the compensation temperature to the isobaric coefficient of thermal expansion α, we have compiled our data and some literature data in *Table 3*. The coefficient of thermal expansion is calculated from the compensation point using $\alpha = (T_c K_c)^{-1}$ with the assumption[24,53] that $K_c = 4$, and compared to the thermal expansion coefficient measured independently for liquids (α_l) and glasses (α_s). A reasonable correlation between $\alpha = (4T_c)^{-1}$ and α_l is seen in *Table 3* considering some of the inaccuracies in the determination of α_l. For solids, it is evident that no single value of K_c will lead to agreement of the calculated expansion coefficient with α_s. In the case of the liquid, the agreement may be fortuitous because the values of α_l do not span a very wide range of values. Also, it is evident that the compensation temperature generally occurs just above T_g and it is known that $\alpha_l T_g = 0.2$ from empirical correlations[55] so the trend in *Table 3* may simply be a result of this relationship.

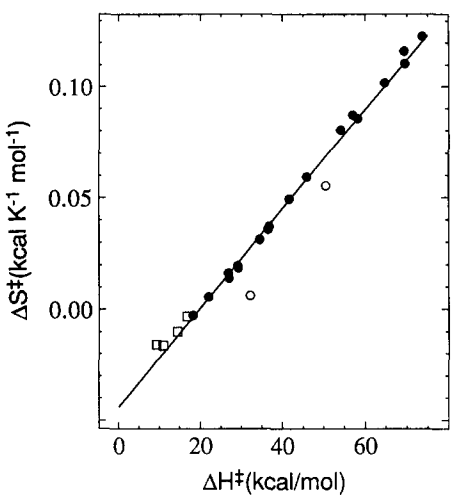

Figure 22 Activated states entropy ($\Delta S^{\ddagger}$) plotted *versus* the entropy ($\Delta H^{\ddagger}$) for PMMA. The linear points indicate the region of compensation. Ranges of T_p (°C): □, −100 to −20; ●, 0–110; ○, 120–130

Other interpretations of $\Delta S^{\ddagger}$ *versus* $\Delta H^{\ddagger}$ have been proposed[52] in terms of the difference in the coefficient of thermal expansion ($\Delta\alpha = \alpha_l - \alpha_s$) above and below T_g. To account for restricted rotation around the chain axis, an extra enthalpy term has been introduced[52] ($\Delta H_{tor}^{\ddagger}$) giving an expression which accounts for the non-zero intercept in the $\Delta S^{\ddagger}$ *versus* $\Delta H^{\ddagger}$ plot[48]:

$$\Delta H^{\ddagger} = (9\Delta\alpha)^{-1}\Delta S^{\ddagger} + \Delta H_{tor}^{\ddagger} = T_c\Delta S^{\ddagger} + \Delta H_{tor}^{\ddagger} \quad (20)$$

and relates $\Delta S^{\ddagger}/\Delta H^{\ddagger}$ to $\Delta\alpha$. It is known empirically[55] that $\Delta\alpha \approx 3.4 \times 10^{-4}\ K^{-1}$ for most polymers and also that $\Delta\alpha T_g = \text{constant} = 0.11$. These are both roughly verified by the independently measured values of $\Delta\alpha$ presented in *Table 4*, although for a wide enough temperature range one of these relationships must fail. The values of $\Delta\alpha$ calculated from the compensation data using equation (20) seem to deviate slightly from those measured independently. Since both $\Delta\alpha$ and the compensation temperature [$T_c = 1/(9\Delta\alpha)$] vary in a fashion similar to T_g, it is difficult to assess the usefulness of equation (20).

Relationship to cooperative relaxations at $T \leqslant T_g$. There is no question that compensation is a manifestation of the significant increase in the values of E_a as one approaches T_g. This increase is concurrent with a departure from the zero activation entropy line. Various theories of the glass transition are available to describe deviations from Arrhenius behaviour and the very large values of E_a which occur at T_g. Some of the more intuitive discussion revolves around the configurational entropy theories[22–24]. These theories suggest that in the equilibrium state above T_g the cooperatively moving unit is largest at T_g and smaller at higher temperatures because more configurations (more free volume) are available.

Table 4 Relationship of compensation temperature to the difference in thermal expansion coefficient across T_g

	τ_c (s)	T_c (°C)	α_s $\times 10^4(K^{-1})$	α_l $\times 10^4(K^{-1})$	$\Delta\alpha = \alpha_l - \alpha_s$ $\times 10^4(K^{-1})$	$\Delta\alpha = 1/(9T_c)^a$ $\times 10^4(K^{-1})$
PEMA	6.8×10^{-3}	108 ± 5	3.1[b]	6.5[c]	3.4	2.9
PMMA	1.6×10^{-3}	165 ± 5	2.7[b]	5.9[c]	3.2	2.5
LCP1[d]	2.75×10^{-6}	188	1.56[d]	4.9[d]	3.34	2.4

[a] $\Delta\alpha = 1/(9T_c)$ where T_c is in K
[b] Ref. 55
[c] Ref. 56
[d] Unpublished t.s.c. data and ref. 57

In the non-equilibrium glassy state below T_g, predictions can also be made of the cooperativity[25]. The theories suggest that the structural state in the glass should give rise to an Arrhenius dependence of relaxation times with the values of E_a increasing with temperature as the glassy structure approaches equilibrium at T_g where the maximum value of E_a is attained. Thus, this type of structural change in the non-equilibrium state can qualitatively explain the increasing values of E_a as one approaches T_g from the low T side and, at the same time, provides an explanation for compensation.

The non-equilibrium glassy state is difficult to model quantitatively but gross effects can be discussed here such as the difference between the methacrylates as compared to the other polymers. Significant departure of E_a from the zero entropy curve occurs at least 60°C below T_g for PEMA and PMMA while for PC, PS and PAR no departure is seen until ~10–25°C below T_g. The reasons for these differences are not entirely clear but we propose that they may be due to structural heterogeneity in the glassy state well below T_g for PEMA and PMMA. It is well known that conventional PMMA is ~80% syndiotactic and ~20% isotactic. Pure syndiotactic PMMA has a T_g of 130°C (ref. 32) and isotactic PMMA has a T_g ≈40°C (ref. 14). Isotactic PMMA has a T_g ~ 65°C lower than conventional PMMA (105°C) so it is possible that, at a microscopic level, a certain population of isotactic sequences is relaxing in a cooperative fashion, while overall the macroscopic structure is more representative of a glassy solid. We have found that the t.s. spectra are very sensitive to cooperative relaxations even if they are a minor component of the total relaxing species, so it is not surprising that the effect is so strong in PMMA. Another semi-microscopic method, such as dynamic mechanical relaxation, shows an interesting difference in modulus (G') between PMMA and polymers such as PS or PC. Values of G' for PS and bisphenol-A PC are typical of most amorphous polymers with almost no change until the very sharp drop in modulus starting at ~10°C below T_g, while for PMMA the modulus decreases at least 200% from 15 to 95°C before dropping sharply just before T_g (ref. 14). Further t.s.c. and mechanical relaxation experiments on a pure syndiotactic PMMA will provide further insight to this issue.

CONCLUSIONS

Thermally stimulated current depolarization (t.s.c.) was used to study relaxations in amorphous polymers over a temperature range covering the β and α (T_g) relaxations. The T_g values determined by t.s.c. were found to be identical with those determined by d.s.c. The β relaxations in PEMA and PMMA were well separated from T_g due to the low equivalent frequency of t.s.c. while they overlap in higher frequency a.c. dielectric measurements. A.c. dielectric studies of the β relaxation in PC resulted in an apparent activation energy which was consistent with that obtained by thermal peak cleaning of the global t.s.c. spectra. Significant curvature was seen in the Arrhenius relaxation map of the α transition in PC and PS due to WLF curvature. The estimated values of E_a were in qualitative agreement with those obtained by t.s.c. at T_g, as were the values of E_a at T_g for PEMA and PMMA when compared with literature values. The agreement of E_a in the low temperature secondary relaxation region with the $\Delta S^{\ddagger} = 0$ activated states prediction, illustrates the localized non-cooperative nature of these relaxations. At higher temperatures, the measured values of E_a depart from the $\Delta S^{\ddagger} = 0$ prediction and exhibit a sharp maximum at T_g. This is a well known feature of glass transitions[14] and is attributed to an enhanced degree of cooperativity in the motions at T_g in light of the theory of Adam and Gibbs[22]. The value of the t.s.c. thermal sampling method is that activation energies can be determined with a very high sensitivity and a temperature resolution generally better than a few degrees. Having a very sensitive probe for detecting cooperative relaxations can be very important in multiphase systems or materials with very weak glass transitions. An example of the need for sensitivity is the case of PEMA and PMMA which showed a substantial amount of cooperative relaxations more than 60°C below T_g while the other polymers studied showed no such effect. Conventional PMMA is ~20% isotactic and isotactic PMMA is known to have a glass transition ~65°C lower than conventional PMMA. It is proposed that in these materials, well below the nominal T_g, there is a small population of cooperatively relaxing species.

Compensation of the t.s.c. relaxation spectra plotted in Arrhenius or Eyring plots was found for all polymers to differing degrees. We have applied the relationship used by Eby[26] relating the slope of a plot of the activation entropy *versus* enthalpy to the isobaric coefficient of thermal volume expansion (α_l) of the polymer liquid. Some qualitative agreement was found, but because of the relationship[55] of $1/\alpha_l$ to T_g and the narrow range of temperatures studied here, the agreement may be fortuitous.

ACKNOWLEDGEMENTS

Discussions with H. W. Starkweather, G. W. Scherer, D. J. Walsh, R. M. Ikeda, S. R. Lustig, L. L. Berger and S. Mazur were most beneficial. The authors thank N. V. DiPaolo, J. R. Dowell and W. G. Kampert for help with the experiments, H. W. Starkweather Jr for the dynamic mechanical data, and D. J. Walsh for supplying the pressure–volume–temperature data from which the thermal expansion coefficients of some of the materials were obtained and for donating the PEMA.

REFERENCES

1 Bernes, A., Boyer, R. F., Chatain, D., Lacabanne, C. and Ibar, J. P. in 'Order in the Amorphous State of Polymers' (Ed. S. E. Keinath), Plenum Press, London, 1987, p. 305
2 Ronarc'h, D., Audren, P. and Moura, J. L. *J. Appl. Phys.* 1985, **58**, 466
3 Ronarc'h, D., Audren, P. and Moura, J. L. *J. Appl. Phys.* 1985, **58**, 474
4 del Val, J. J., Alegria, A., Colmenero, J. and Lacabanne, C. *J. Appl. Phys.* 1986, **59**, 3829
5 del Val, J. J., Lacabanne, C. and Hiltner, A. *J. Appl. Phys.* 1988, **63**, 5312
6 Fraile, J., Torres, A., Jiménez, J. and de Saja, J. A. *Polymer* 1989, **30**, 1977
7 Sharif Faruque, H. and Lacabanne, C. *J. Mater. Sci.* 1990, **25**, 321
8 Migahed, M. D., El-Khodary, A., Hammam, M., Shaban, A. and Hafiz, H. R. J. *J. Mater. Sci.* 1990, **25**, 2795
9 Sauer, B. B., Avakian, P. and Cohen, G. M. *Polymer* 1992, **33**, 2666
10 Crevecoeur, G. and Groeninckx, G. *Macromolecules* 1991, **24**, 1190
11 Kenny, J., D'Amore, A., Nicolais, L., Iannone, M. and Scatteia, B. *SAMPE J.* 1989, **25**, 27

12 Goodwin, A. A. and Hay, J. N. *Polym. Commun.* 1989, **30**, 288
13 Sauer, B. B., Avakian, P., Hsiao, B. S. and Starkweather, H. W. *Macromolecules* 1990, **23**, 5119
14 McCrum, N. H., Read, B. E. and Williams, G. 'Anelastic and Dielectric Effects in Polymeric Solids', Wiley, New York, 1967
15 Starkweather, H. W. Jr *Macromolecules* 1988, **21**, 1798
16 Krug, R. R., Hunter, W. G. and Grieger, R. A. *J. Phys. Chem.* 1976, **80**, 2335
17 Lacabanne, C., Chatain, D., Monpagens, J. C., Hiltner, A. and Baer, E. *Solid State Commun.* 1978, **27**, 1055
18 McCrum, N. G. *Polymer* 1984, **25**, 299
19 Demont, P., Chatain, D., Lacabanne, C., Ronarc'h, D. and Moura, J.-L. *Polym. Eng. Sci.* 1984, **24**, 127
20 Lacabanne, C., Chatain, D., Monpagens, J. C. and Berticat, Ph. *J. Appl. Phys.* 1979, **50**, 2723
21 Read, B. E. *Polymer* 1989, **30**, 1439
22 Adam, G. and Gibbs, J. H. *J. Chem. Phys.* 1965, **43**, 139
23 Matsuoka, S., Johndon, G. E., Illiams, G. and Bair, H. E. *Macromolecules* 1985, **18**, 2652
24 Matsuoka, S. Proceedings 18th NATAS Conference (Ed. I. R. Harrison), 1989, p. 125
25 Scherer, G. W. *J. Am. Chem. Soc.* 1984, **67**, 504
26 Eby, R. K. *J. Chem. Phys.* 1962, **37**, 2785
27 Fischer, P. and Röhl, P. *J. Polym. Sci., Polym. Phys. Edn* 1976, **14**, 531
28 Fischer, P. and Röhl, P. *J. Polym. Sci., Polym. Phys. Edn* 1976, **14**, 543
29 Simon, G. P. *Polymer* 1989, **30**, 2227
30 Zielinski, M., Swiderski, T. and Kryszewski, M. *Polymer* 1978, **19**, 883
31 Jarrigeon, M., Chabert, B., Chatain, D., Lacabanne, C. and Nemoz, G. *J. Macromol. Sci., Phys.* 1980, **B17**, 1
32 Gourari, A., Bendaoud, M., Lacabanne, C. and Boyer, R. F. *J. Polym. Sci., Polym. Phys. Edn* 1985, **23**, 889
33 Chatain, D., Gautier, P. and Lacabanne, C. *J. Polym. Sci., Polym. Phys. Edn* 1973, **11**, 1631
34 van Turnhout, J. *Polym. J.* 1971, **2**, 173
35 van Turnhout, J. 'Thermally Stimulated Discharge of Polymer Electrets', Elsevier, Amsterdam, 1975
36 van Turnhout, J. in 'Topics in Applied Physics, Vol. 33, Electrets' (Ed. G. M. Sessler), Springer Verlag, Berlin, 1980, p. 81
37 Bucci, C., Fieschi, R. and Guidi, G. *Phys. Rev.* 1966, **148**, 816
38 Fröhlich, H. 'Theory of Dielectrics', Clarendon Press, Oxford, 1949
39 Figueroa, D. R., Fontanella, J. J., Wintersgill, M. C., Calame, J. P. and Andeen, C. G. *Solid State Ionics* 1988, **28**, 1023
40 Wissler, G. E. and Crist, B. *J. Polym. Sci., Polym. Phys. Edn* 1980, **18**, 1257
41 Vanderschueren, J., Linkens, A., Haas, B. and Dellicour, E. *J. Macromol. Sci., Phys.* 1978, **B15**, 449
42 Boyer, E. F. *J. Macromol. Sci., Phys.* 1980, **B18**, 461
43 Kumler, P. L., Machajewski, G. A., Fitzgerald, J. J., Denny, L. R., Keinath, S. E. and Boyer, R. F. *Macromolecules* 1987, **20**, 1060
44 Hoffman, J. D., Williams, G. and Passaglia, E. *J. Polym. Sci. C* 1966, **14**, 211
45 Jonscher, A. K. in 'Dielectric Relaxation in Solids', Chelsea Dielectrics Press, London, 1983, pp. 263–265
46 Scherer, G. Personal communication, 1991
47 Saito, S. and Nakajima, T. *J. Appl. Polym. Sci.* 1959, **2**, 93
48 Starkweather, H. W. *Macromolecules* 1981, **14**, 1277
49 Ishida, Y. and Yamafuji, K. *Kolloid Z.* 1961, **177**, 97
50 Broens, O. and Müller, F. H. *Kolloid Z.* 1955, **140**, 121
51 Broens, O. and Müller, F. H. *Kolloid Z.* 1955, **141**, 20
52 Isoda, S. and Asai, K. *Jpn J. Appl. Phys.* 1974, **13**, 1333
53 Keyes, R. W. *J. Chem. Phys.* 1958, **29**, 467
54 Crine, J.-P. *J. Appl. Phys.* 1989, **66**, 1308
55 Van Krevelen, D. W. in 'Properties of Polymers, their Estimation and Correlation with Chemical Structure', Elsevier, Amsterdam, 1976, pp. 70–73
56 Walsh, D. J. Unpublished data
57 Walsh, D. J., Dee, G. T. and Wojtkowski, P. W. *Polymer* 1989, **30**, 1467